Obesity-Induced Increase in Cystatin C Alleviates Tissue Inflammation

Dedual, Mara A ; Wueest, Stephan ; Challa, Tenagne D ; Lucchini, Fabrizio C ; Aeppli, Tim R J ; Borsigova, Marcela ; Mauracher, Andrea A ; Vavassori, Stefano ; Pachlopnik Schmid, Jana ; Blüher, Matthias ; Konrad, Daniel

Abstract: We recently demonstrated that removal of one kidney (uninephrectomy; UniNx) in mice reduced high fat-diet (HFD)-induced adipose tissue inflammation thereby improving adipose tissue and hepatic insulin sensitivity. Of note, circulating cystatin C (CysC) levels were increased in UniNx compared to sham-operated mice. Importantly, CysC may have anti-inflammatory properties, and circulating CysC levels were reported to positively correlate with obesity in humans and as shown herein in HFD-fed mice. However, the causal relationship of such observation remains unclear. HFD feeding of CysC-deficient (CysC KO) mice deteriorated obesity-associated adipose tissue inflammation and dysfunction, as assessed by pro-inflammatory macrophage accumulation. In addition, mRNA expression of pro-inflammatory mediators was increased, whereas markers of adipocyte differentiation were decreased. Similarly to findings in adipose tissue, expression of pro-inflammatory cytokines was increased in liver and skeletal muscle of CysC KO mice. In line, HFD-induced hepatic insulin resistance and impairment of glucose tolerance were further aggravated in knockout mice. Consistently, chow-fed CysC KO mice were more susceptible to lipopolysaccharide (LPS)-induced adipose tissue inflammation. In people with obesity, circulating CysC levels correlated negatively with adipose tissue Hif1 as well as IL-6 mRNA expression. Moreover, healthy (i.e. insulin-sensitive) subjects with obesity depicted significantly higher mRNA expression of CysC in white adipose tissue. In conclusion, CysC is upregulated under obesity conditions and thereby counteracts inflammation of peripheral insulin-sensitive tissues and, thus, obesity-associated deterioration of glucose metabolism.

DOI: https://doi.org/10.2337/db19-1206

Obesity-Induced Increase in Cystatin C Alleviates Tissue Inflammation

Mara A. Dedual[1,2,3], Stephan Wueest[1,2], Tenagne D. Challa[1,2], Fabrizio C. Lucchini[1,2], Tim R. J. Aeppli[1,2], Marcela Borsigova[1,2], Andrea A. Mauracher[2,4], Stefano Vavassori[2,4], Jana Pachlopnik Schmid[2,4], Matthias Blüher[5], Daniel Konrad[1,2,3]

[1]Division of Pediatric Endocrinology and Diabetology and [2]Children's Research Center, University Children's Hospital, CH-8032 Zurich, Switzerland

[3]Zurich Center for Integrative Human Physiology, University of Zurich, CH-8057 Zurich, Switzerland

[4]Division of Pediatric Immunology, University Children's Hospital, CH-8032 Zurich, Switzerland

[5]Department of Medicine, Endocrinology and Diabetes, University of D-04103 Leipzig, Germany

Lead contact:

Daniel Konrad, MD PhD

University Children's Hospital

Department of Endocrinology and Diabetology

Steinwiesstrasse 75

CH-8032 Zurich

Tel: ++41-44-266 7966; Fax: ++41-44-266 7983

Email: daniel.konrad@kispi.uzh.ch

Diabetes Publish Ahead of Print, published online July 2, 2020

Abstract

We recently demonstrated that removal of one kidney (uninephrectomy; UniNx) in mice reduced high fat-diet (HFD)-induced adipose tissue inflammation thereby improving adipose tissue and hepatic insulin sensitivity. Of note, circulating cystatin C (CysC) levels were increased in UniNx compared to sham-operated mice. Importantly, CysC may have anti-inflammatory properties, and circulating CysC levels were reported to positively correlate with obesity in humans and as shown herein in HFD-fed mice. However, the causal relationship of such observation remains unclear. HFD feeding of CysC-deficient (CysC KO) mice deteriorated obesity-associated adipose tissue inflammation and dysfunction, as assessed by pro-inflammatory macrophage accumulation. In addition, mRNA expression of pro-inflammatory mediators was increased, whereas markers of adipocyte differentiation were decreased. Similarly to findings in adipose tissue, expression of pro-inflammatory cytokines was increased in liver and skeletal muscle of CysC KO mice. In line, HFD-induced hepatic insulin resistance and impairment of glucose tolerance were further aggravated in knockout mice. Consistently, chow-fed CysC KO mice were more susceptible to lipopolysaccharide (LPS)-induced adipose tissue inflammation. In people with obesity, circulating CysC levels correlated negatively with adipose tissue *Hif1α* as well as *IL-6* mRNA expression. Moreover, healthy (i.e. insulin-sensitive) subjects with obesity depicted significantly higher mRNA expression of *CysC* in white adipose tissue.

In conclusion, CysC is upregulated under obesity conditions and thereby counteracts inflammation of peripheral insulin-sensitive tissues and, thus, obesity-associated deterioration of glucose metabolism.

Introduction

Obesity-induced inflammation is a crucial driver of insulin resistance and type 2 diabetes. In obesity, white adipose tissue (WAT) expansion is associated with local infiltration of pro-inflammatory cells, with macrophages being the quantitatively predominant cell type. The latter accounts for a large proportion of adipose tissue-derived pro-inflammatory proteins such as IL-1β, IL-6, TNFα or hypoxia-inducible factor-1α (HIF1α) (1), altering the secretory pattern of adipocytes. Consequently, the release of pro-inflammatory cytokines and free fatty acids (FFA) is increased contributing to the vicious circle of obesity-associated chronic low grade inflammation locally as well as systemically, e.g. in the liver and in skeletal muscle (2, 3). Due to the central role of inflammation in the pathogenesis of type 2 diabetes, identification of anti-inflammatory targets to combat insulin resistance and its related co-morbidities are warranted (4).

We previously found that removal of one kidney (uninephrectomy; UniNx) in obese mice ameliorates obesity-induced adipose tissue and liver inflammation (5, 6). Cystatin C (CysC) is a marker of the glomerular filtration rate (7) and increased in patients with renal failure (8). Since CysC was previously reported to have immunomodulatory function, we hypothesized that increased circulating CysC levels contributed to the blunted inflammation in UniNx mice. CysC was found to be internalized into lipopolysaccharide (LPS)-stimulated monocytes and to downregulate the production of pro-inflammatory cytokines such as TNFα or IL-1β (9). Moreover, an association between elevated circulating CysC levels and type 2 diabetes has been reported (10, 11). However, the pathophysiological implication of such association remains to be elucidated. Herein, we propose that elevated CysC levels in obesity counterbalance obesity-associated inflammation thereby restoring glucose tolerance.

Research Design and Methods

Human Studies

Serum concentration of CysC, IL-10 and lipocalin-2 as well as mRNA expression in subcutaneous or visceral WAT were determined in 63 individuals (age 19-82 years; BMI 25-75 kg/m²) who underwent laparoscopic sleeve gastrectomy, cholecystectomy, hernia or Roux-en-Y gastric bypass surgery. In addition, CysC mRNA expression in subcutaneous WAT was analyzed in a previously described subgroup of individuals with either insulin-sensitive (n=30) or insulin-resistant obesity (n=30) (12). All investigations were approved by the ethics committee of the University of Leipzig (# 159-12-21052012) and were carried out in accordance with the Declaration of Helsinki. All participants provided witnessed written informed consent before study entrance. mRNA expression was measured by qRT-PCR using Assay-on-Demand gene expression kit and calculated relative to the expression of *HPRT1* mRNA. For primer details see Supplementary Tab. 1.

Animals

CysC-deficient mice (13) were bred to C57BL/6J wildtype mice to eventually obtain homozygous CysC KO and (wild-type) WT littermates.

Mice were housed in a pathogen-free environment with an alternating 12 h dark and light cycle. Six-week old male WT and CysC KO mice were fed *ad libitum* either a regular chow (ProvimiKliba) or a HFD (59 kcal% fat, D12331 mod. Surwit, ssniff Spezialdiäten GmbH, for 20 weeks. All protocols conformed to the Swiss animal protection laws and were authorized by the Cantonal Veterinary Office in Zurich, Switzerland.

Intraperitoneal glucose and insulin tolerance tests

Glucose and insulin tolerance were assessed as described (14).

Hyperinsulinemic-euglycemic clamp studies

Hyperinsulinemic-euglycemic clamp studies were performed as described before (15).

Metabolic cage analysis

Energy expenditure, locomotor activity and food intake were assessed in 24-hour single-housed mice using the PhenoMaster system (TSE Systems).

Determination of plasma parameters

Free fatty acid (FFA) concentrations were determined using an enzymatic colorimetric assay (Wako Chemicals GmbH). Plasma CysC (BioVendor) and insulin (Crystal Chem) levels were measured using ELISA kits.

Adipocyte size determination

Distribution of adipocyte diameter was determined by the MultisizerTM 3 Coulter Counter (Beckman Coulter Life Sciences).

Real time quantitative PCR

cDNA was amplified using TaqMan assays (Applied Biosystems) and normalized to 18s RNA using the $2^{-\Delta\Delta CT}$ method. For primer details see Supplementary Tab. 2.

Western Blotting

Western blots were obtained as described (14). For antibody details see Supplementary Tab. 3.

Flow cytometry

Stromal-vascular fraction of eWAT was collected as described (16). For staining details see Supplementary Tab. 4. Measurements were performed with a flow cytometer (Beckman Coulter), and data were analyzed with FlowJo software. Relative frequency of single, live lymphocytes of the respective subpopulation was assessed.

Osmotic mini-pump experiments

Osmotic mini-pump (Alzet Model 1004) was implanted into the intraperitoneal cavity of anesthetized 12-week old mice. Mini-pumps were filled with LPS from Escherichia coli (055:B5, Sigma) to infuse 300 µg/kg*day for four weeks.

Data analysis

Data were analyzed by Spearman correlation, unpaired, two-tailed Student's t-test or by one- or two-way analysis of variance (ANOVA) followed by Bonferroni post-hoc test.

Data and Resource Availability

All data generated or analyzed during this study are included here (and in Supplementary Data) or are available from the corresponding author upon reasonable request.

Results

Higher degree of adiposity in HFD-fed CysC KO mice

First, we explored the effect of HFD-feeding on circulating CysC levels in WT mice. As depicted in Fig. 1A, 20 weeks of HFD increased plasma CysC concentrations in systemic and portal (Supplementary Fig. 1A) blood compared to age-matched chow-fed mice independently of kidney function since plasma creatinine levels were similar among chow- and HFD-fed WT mice (Supplementary Fig. 1B). Moreover, CysC plasma levels were significantly increased in HFD-fed UniNx compared to sham-operated mice (Fig. 1B). Of note, UniNx had a protective effect on HFD-induced adipose tissue inflammation and hepatic insulin resistance (5). To explore a potential role of increased CysC on adipose tissue function, we analyzed CysC KO mice (13). As expected, CysC was absent in the circulation of CysC KO mice (Fig. 1C). CysC KO mice exhibited lower body weight under chow-diet whereas it was no longer different in HFD-fed mice (Fig. 1D). Furthermore, mass of inguinal and mesenteric fat depots was significantly increased in HFD-fed knockout mice (Fig. 1E). Such increased fat accumulation might be due to a pronounced positive energy balance since we observed diminished locomotor activity and decreased energy expenditure in HFD-fed CysC KO mice that may have outweighed lower food intake in these mice (Supplementary Fig. 2). Of note, whereas energy expenditure was similarly decreased in chow-fed CysC KO mice, their locomotor activity and food intake were not different when compared to WT mice (Supplementary Fig. 3).

In inguinal WAT (iWAT) of HFD-fed mice, levels of the adipocyte differentiation markers PPARγ and CEBPβ were decreased (Figs. 1F and G). Consistently, adipocyte size was enlarged in HFD-fed CysC KO mice (Fig. 1H). In contrast, PPARγ and CEBPβ

protein levels were similar in iWAT of chow-fed WT and CysC KO mice (Supplementary Fig. 4A). Moreover, recombinant CysC treatment did not affect differentiation of 3T3-L1 adipocytes (Supplementary Fig. 4B), indicating that CysC has no direct effect on the latter. Obesity-associated adipose tissue dysfunction is accompanied by impaired angiogenesis (17). In accordance, levels of the pro-angiogenic protein vascular endothelial growth factor (VEGF) were decreased in iWAT of HFD-fed CysC KO mice (Supplementary Fig. 5A). Similarly, VEGF protein levels were decreased in skeletal muscle (Supplementary Fig. 5B). Taken together, lack of CysC aggravates HFD-induced adiposity and reduces adipocyte differentiation markers consistent with adipose tissue dysfunction in these mice.

Pronounced obesity-induced impairment of glucose metabolism in CysC KO mice

Glucose metabolism was assessed next in chow- and HFD-fed CysC KO and WT mice. Whereas CysC KO mice were slightly more glucose tolerant under chow diet, glucose tolerance was further deteriorated in HFD-fed CysC KO compared to WT mice (Figs. 2A-C). Accordingly, the negative impact of HFD on glucose tolerance was significantly more pronounced in CysC KO mice (Fig. 2D). Insulin tolerance was increased in chow-fed but similar in HFD-fed CysC KO mice when compared to WT mice (Supplementary Figs. 6A-D). Circulating insulin levels were similar in both genotypes under both diets (Supplementary Fig. 6E). Hyperinsulinemic-euglycemic clamp studies revealed similar glucose infusion rate reflecting similar whole-body insulin sensitivity in HFD-fed CysC KO and WT mice (Fig. 2E). In contrast, endogenous glucose production was significantly higher in CysC KO mice (Fig. 2F) indicating impaired hepatic insulin sensitivity. Whereas glucose uptake into white adipose tissue depots was comparable between both genotypes, glucose uptake into glycolytic soleus muscle was trend-wise

increased in CysC KO mice (Fig. 2G). Possibly, this increased glucose uptake into soleus counteracted blunted insulin response in the liver, resulting in an overall similar glucose infusion rate (Fig. 2E). Albeit not significantly different, glucose uptake into iWAT was almost 50% lower in CysC KO (Fig. 2G). In addition, insulin's capacity to reduce circulating FFA during clamps was significantly blunted in CysC KO mice (Fig. 2H), suggesting impaired WAT insulin sensitivity. Taken together, CysC KO mice are more susceptible to HFD-induced deterioration of glucose tolerance.

Increased expression of pro-inflammatory cytokines in WAT of HFD-fed and LPS-treated chow-fed CysC KO mice

CysC may have anti-inflammatory properties (9). Consistently, mRNA expression of pro-inflammatory proteins was increased in both iWAT as well as epididymal WAT (eWAT) of HFD-fed CysC KO mice (Figs. 3A and B). In line, infiltration with pro-inflammatory macrophages was enhanced in eWAT of HFD-fed CysC KO compared to WT mice as assessed by flow cytometry (Fig. 3C and Supplementary Fig. 7). Similar to WAT, expression of pro-inflammatory cytokines was increased in liver and skeletal muscle of HFD-fed CysC KO mice (Figs. 3D and E). In contrast, mRNA expression of these cytokines was not different between both genotypes under chow diet (Supplementary Fig. 8).

To explore whether chow-fed CysC KO mice were more susceptible to exogenous pro-inflammatory stimuli, LPS, which was demonstrated to promote adipose tissue inflammation in lean mice (18), was chronically administrated to chow-fed CysC KO and WT mice using mini-pumps. We hypothesized that an isolated increase in circulating LPS levels would aggravate adipose tissue inflammation in chow-fed mice lacking the

protective effect of CysC. Indeed, adipose tissue inflammation was pronounced in lean CysC KO mice, as demonstrated by increased mRNA expression of *IL-6* (Fig. 3F). In line, phosphorylation of IL-6 downstream targets such as STAT3 and ERK 1/2 were increased in CysC KO mice (Supplementary Fig. 9).

CysC can be internalized into LPS-stimulated macrophages thereby downregulating the expression and secretion of pro-inflammatory cytokines (9, 19). CysC-treatment of LPS-stimulated RAW cells decreased mRNA expression of *Hif1α* (Fig. 3G), which has been previously linked to adipose tissue inflammation (20). In parallel, the release of TNFα and MCP1 was reduced (Supplementary Fig. 10). To test potential anti-inflammatory properties of CysC in obesity-associated adipose tissue inflammation, eWAT explants of HFD-fed mice were incubated with or without recombinant CysC. Importantly, CysC-treatment significantly reduced *Hif1α* mRNA levels in eWAT explants (Fig. 3H). In addition, *Vegf-A* mRNA expression was upregulated in response to CysC-treatment (Supplementary Fig. 11).

Taken together, CysC modulates inflammation in insulin-sensitive tissues in mice.

Negative correlation of circulating CysC levels with inflammation markers in human WAT

Consistent to observation in rodents (Fig. 3A), circulating CysC levels correlated negatively with *HIF1α* (Fig. 4A) and *TNFα* (Fig. 4B) mRNA expression in subcutaneous white adipose tissue of human subjects. Similarly, *HIF1α* and *IL-6* mRNA expression in visceral WAT associated negatively with serum CysC concentration (Figs. 4C and D). Moreover, the latter correlated negatively with the pro-inflammatory protein lipocalin-2 (Fig. 4E), but positively with the anti-inflammatory cytokine IL-10 (Fig. 4F). In further support of anti-inflammatory properties of CysC, healthy i.e. insulin-sensitive obese

subjects depicted higher *CysC* mRNA expression in subcutaneous WAT than insulin-resistant obese patients (Fig. 4G).

Discussion

The current study shows that elevated circulating CysC levels in obesity reduce (adipose) tissue inflammation and, thus, has a beneficial impact on glucose tolerance. Circulating CysC is not only increased in kidney failure, but also in obese humans and mice (21, 22). Consistently, we found increased circulating CysC levels in uninephrectomized as well as in HFD-fed mice. Of note, WAT from obese humans revealed higher expression and secretion of CysC, suggesting a direct contribution of WAT to obesity-associated increase in circulating CysC (23). Similarly, murine WAT expresses significant amounts of CysC (24), supporting the notion that WAT is as an important source of circulating CysC levels.

In support of the suggested anti-inflammatory properties of CysC, its circulating levels correlated negatively with inflammatory markers in human subcutaneous and visceral WAT and, additionally, CysC-treatment reduced inflammatory markers in murine fat explants. Moreover, lack of CysC promotes an aggravation of HFD-induced WAT, liver and skeletal muscle inflammation in mice as determined by mRNA expression of pro-inflammatory cytokines and accumulation of pro-inflammatory macrophages in WAT. A putative role of obesity-associated macrophage accumulation as a major cytokine source and, hence, as driver of WAT inflammation has been suggested before (1). CysC may inhibit secretion of pro-inflammatory cytokines by LPS-stimulated macrophages (9). Consistently, we found herein that LPS-mediated WAT inflammation was aggravated in

lean CysC-deficient mice, suggesting a direct immunomodulatory effect of CysC on WAT inflammation. In the latter experiment, chronically LPS-treated CysC KO mice displayed not only pronounced *IL-6* upregulation but also increased activation of its downstream targets STAT3 and ERK 1/2 when compared to WT mice. Of note, a regulatory effect of CysC on LPS-stimulated ERK 1/2-phosphorylation has been reported in human monocytes before (9).

Obesity-associated WAT inflammation may inhibit adipogenesis resulting in adipocyte hypertrophy (17, 20). In fact, inflammatory mediators such as IL-6 and TNFα that are both elevated in WAT of HFD-fed KO mice may negatively affect adipocyte differentiation and/or induce de-differentiation of white adipocytes (25, 26). In support of such notion, elevated *Il-6* and *Tnfα* expression observed in HFD-fed CysC-deficient mice was associated with diminished protein levels of the adipocyte differentiation factors PPARγ and CEBPβ as well as hypertrophied adipocytes further supporting our hypothesis that CysC elicits anti-inflammatory properties and, thus, may counteract WAT inflammation. Moreover, we observed decreased levels of the pro-angiogenic protein VEGF-A, which is important for healthy WAT expansion and vascularization (17), in WAT of HFD-fed CysC KO mice. Consistently, CysC has been reported to increase VEGF (27). These findings further support a beneficial role of CysC in adipose tissue of obese.

In conclusion, increased CysC in obesity may counterbalance obesity-associated inflammation and, thus, protects from additional obesity-associated deterioration of glucose homeostasis. Besides elevated inflammation, increased HFD-induced body weight gain and/or impaired vascularization may contribute to impaired glucose tolerance in HFD-fed Cys C KO mice.

Grants

This work was supported by grants from the Wolfermann-Nägeli Foundation, the Children's Research Centre, University Children's Hospital Zurich, and the Forschungskredit "candoc", University of Zurich (#FK-18-027) (all to MAD) as well as from the Swiss National Science Foundation (#310030-160129 and #310030-179344 to DK).

Author Contributions

M.A.D. designed and performed experiments, analyzed data and wrote the manuscript. S. W. designed and performed experiments. T. D. C., F. C. L., T. R. J. A., M. Bo., A. A. M. and S. V. performed experiments. J. P. S. designed experiments. M. Bl. provided human samples and designed experiments. D.K. designed experiments, analyzed data and wrote the manuscript. All authors reviewed and commented on the manuscript.

D.K. is the guarantor of this work and, as such, had full access to all the data in the study and takes responsibility for the integrity of the data and the accuracy of the data analysis.

Declaration of Interests

The authors declare no conflict of interests.

References

1. Weisberg SP, McCann D, Desai M, Rosenbaum M, Leibel RL, Ferrante AW, Jr. Obesity is associated with macrophage accumulation in adipose tissue. J Clin Invest. 2003;112(12):1796-808.
2. Shulman GI. Ectopic fat in insulin resistance, dyslipidemia, and cardiometabolic disease. N Engl J Med. 2014;371(12):1131-41.
3. Wisse BE. The inflammatory syndrome: the role of adipose tissue cytokines in metabolic disorders linked to obesity. J Am Soc Nephrol. 2004;15(11):2792-800.
4. Donath MY. Targeting inflammation in the treatment of type 2 diabetes: time to start. Nat Rev Drug Discov. 2014;13(6):465-76.
5. Chin SH, Item F, Wueest S, Zhou Z, Wiedemann MS, Gai Z, et al. Opposing effects of reduced kidney mass on liver and skeletal muscle insulin sensitivity in obese mice. Diabetes. 2015;64(4):1131-41.
6. Gai Z, Hiller C, Chin SH, Hofstetter L, Stieger B, Konrad D, et al. Uninephrectomy augments the effects of high fat diet induced obesity on gene expression in mouse kidney. Biochim Biophys Acta. 2014;1842(9):1870-8.
7. Lafarge JC, Naour N, Clement K, Guerre-Millo M. Cathepsins and cystatin C in atherosclerosis and obesity. Biochimie. 2010;92(11):1580-6.
8. Komura N, Kihara S, Sonoda M, Maeda N, Tochino Y, Funahashi T, et al. Increment and impairment of adiponectin in renal failure. Cardiovasc Res. 2010;86(3):471-7.
9. Gren ST, Janciauskiene S, Sandeep S, Jonigk D, Kvist PH, Gerwien JG, et al. The protease inhibitor cystatin C down-regulates the release of IL-beta and TNF-alpha in lipopolysaccharide activated monocytes. J Leukoc Biol. 2016;100(4):811-22.
10. Donahue RP, Stranges S, Rejman K, Rafalson LB, Dmochowski J, Trevisan M. Elevated cystatin C concentration and progression to pre-diabetes: the Western New York study. Diabetes Care. 2007;30(7):1724-9.
11. Sahakyan K, Lee KE, Shankar A, Klein R. Serum cystatin C and the incidence of type 2 diabetes mellitus. Diabetologia. 2011;54(6):1335-40.
12. Kloting N, Fasshauer M, Dietrich A, Kovacs P, Schon MR, Kern M, et al. Insulin-sensitive obesity. Am J Physiol Endocrinol Metab. 2010;299(3):E506-15.
13. Huh CG, Hakansson K, Nathanson CM, Thorgeirsson UP, Jonsson N, Grubb A, et al. Decreased metastatic spread in mice homozygous for a null allele of the cystatin C protease inhibitor gene. Mol Pathol. 1999;52(6):332-40.
14. Wueest S, Rapold RA, Schumann DM, Rytka JM, Schildknecht A, Nov O, et al. Deletion of Fas in adipocytes relieves adipose tissue inflammation and hepatic manifestations of obesity in mice. J Clin Invest. 2010;120(1):191-202.
15. Challa TD, Wueest S, Lucchini FC, Dedual M, Modica S, Borsigova M, et al. Liver ASK1 protects from non-alcoholic fatty liver disease and fibrosis. EMBO Mol Med. 2019;11(10):e10124.
16. Wueest S, Mueller R, Bluher M, Item F, Chin AS, Wiedemann MS, et al. Fas (CD95) expression in myeloid cells promotes obesity-induced muscle insulin resistance. EMBO Mol Med. 2014;6(1):43-56.
17. Crewe C, An YA, Scherer PE. The ominous triad of adipose tissue dysfunction: inflammation, fibrosis, and impaired angiogenesis. J Clin Invest. 2017;127(1):74-82.
18. Cani PD, Amar J, Iglesias MA, Poggi M, Knauf C, Bastelica D, et al. Metabolic endotoxemia initiates obesity and insulin resistance. Diabetes. 2007;56(7):1761-72.

19. Stralberg F, Kassem A, Kasprzykowski F, Abrahamson M, Grubb A, Lindholm C, et al. Inhibition of lipopolysaccharide-induced osteoclast formation and bone resorption in vitro and in vivo by cysteine proteinase inhibitors. J Leukoc Biol. 2017;101(5):1233-43.
20. Halberg N, Khan T, Trujillo ME, Wernstedt-Asterholm I, Attie AD, Sherwani S, et al. Hypoxia-inducible factor 1alpha induces fibrosis and insulin resistance in white adipose tissue. Mol Cell Biol. 2009;29(16):4467-83.
21. Chew-Harris JS, Florkowski CM, George PM, Elmslie JL, Endre ZH. The relative effects of fat versus muscle mass on cystatin C and estimates of renal function in healthy young men. Ann Clin Biochem. 2013;50(Pt 1):39-46.
22. Ji X, Yao L, Wang M, Liu X, Peng S, Li K, et al. Cystatin C attenuates insulin signaling transduction by promoting endoplasmic reticulum stress in hepatocytes. FEBS Lett. 2015;589(24 Pt B):3938-44.
23. Naour N, Fellahi S, Renucci JF, Poitou C, Rouault C, Basdevant A, et al. Potential contribution of adipose tissue to elevated serum cystatin C in human obesity. Obesity (Silver Spring). 2009;17(12):2121-6.
24. Schmid C, Ghirlanda C, Zwimpfer C, Tschopp O, Zuellig RA, Niessen M. Cystatin C in adipose tissue and stimulation of its production by growth hormone and triiodothyronine in 3T3-L1 cells. Mol Cell Endocrinol. 2019;482:28-36.
25. Almuraikhy S, Kafienah W, Bashah M, Diboun I, Jaganjac M, Al-Khelaifi F, et al. Interleukin-6 induces impairment in human subcutaneous adipogenesis in obesity-associated insulin resistance. Diabetologia. 2016;59(11):2406-16.
26. Coppack SW. Pro-inflammatory cytokines and adipose tissue. Proc Nutr Soc. 2001;60(3):349-56.
27. Dreilich M, Wagenius G, Bergstrom S, Brattstrom D, Larsson A, Hesselius P, et al. The role of cystatin C and the angiogenic cytokines VEGF and bFGF in patients with esophageal carcinoma. Med Oncol. 2005;22(1):29-38.

Figure Legends

Fig. 1 Higher degree of adiposity in HFD-fed CysC KO mice

(A) Plasma levels of CysC in systemic blood of WT mice (n=23 chow-fed mice and n=12 HFD-fed mice). (B) Plasma levels of CysC in systemic blood of HFD-fed UniNx and sham-operated mice (n=6 mice per group). (C) Circulating CysC levels of WT and CysC KO mice (n=4 WT and n=3 CysC KO mice). (D) Weight gain curves of WT and CysC KO mice over 20 weeks of chow- or HFD-feeding (n=35 chow-fed WT and n=29 chow-fed CysC KO, n=25 HFD-fed WT and n=23 HFD-fed CysC KO) are depicted. (E) Weight of white adipose tissue depots of HFD-fed WT and CysC KO mice (n=9 mice per group). Representative Western blots and quantification of protein levels of PPARγ (F) and CEBPβ (G) in iWAT (n=4 WT and n=5 CysC KO). Protein levels were normalized to WT mice. (H) Adipocyte size distribution within iWAT of HFD-fed WT and CysC KO mice. Shown are representative pictures of H&E-stained histological sections (*scale bar*=100 µm) as well as the proportional distribution of different adipocyte size (n=5 WT and n=3 CysC KO). Values are expressed as mean (H) or mean±SEM (A-G). #p=0.09, *p<0.05, **p<0.01. Two-way ANOVA (D), Student's *t*-test (A, B, E-G).

Fig. 2 Pronounced obesity-induced impairment of glucose metabolism in CysC KO mice

(A-C) Intraperitoneal glucose tolerance test (ipGTT) of chow- (n=20 WT and n=19 CysC KO mice) and HFD-fed (n=16 WT and n=12 CysC KO mice) WT and CysC KO mice. (D) HFD-induced increase of area under the curve (AUC) relative to corresponding chow-fed baseline level (n=16 WT and n=12 CysC KO mice). Glucose infusion rate (GIR) (E),

endogenouse glucose production (EGP) (F) and tissue glucose uptake (G) during hyperinsulinemic-euglycemic clamp (n=4 WT and n=5-6 CysC KO mice). (H) Insulin–mediated reduction in circulating FFA levels during hyperinsulinemic-euglycemic clamp (n=3 mice per group). Values are expressed as mean±SEM. #p=0.1, *p<0.05, **p<0.01, ***p<0.001, ****p<0.0001. Student's *t*-test (D-H), two-way ANOVA (A, B), one-way ANOVA (C).

Fig. 3 Increased expression of pro-inflammatory cytokines in WAT of HFD-fed and LPS-treated chow-fed CysC KO mice

mRNA expression of pro-inflammatory markers in iWAT (A; n=7-8 WT and n=6-7 CysC KO mice) and eWAT (B; n=5 WT and n=6-7 CysC KO) of HFD-fed WT and CysC KO mice. (C) Numbers of CD11b+ F4/80+ Ly6G- Ly-6C^{high} macrophages relative to live, single lymphocytes after excluding neutrophils and eosinophils in the stromal vascular fraction of eWAT obtained from HFD-fed WT and CysC KO mice (n= 4 mice per group, 2 independent experiments). mRNA expression of pro-inflammatory cytokines in liver (D; n=5 WT and n=4 CysC KO) and in skeletal muscle (E; n=5 WT and n=6-7 CysC KO) of HFD-fed CysC KO mice are depicted. (F) mRNA expression of pro-inflammatory mediators in eWAT of LPS-infused chow-fed WT and CysC KO mice (n=6 mice per group). (G) mRNA expression of *Hif1α* in LPS-stimulated RAW 264.7 cells in the absence or presence of CysC (n=6 independent experiments). (H) mRNA expression of *Hif1α* in eWAT explants harvested from HFD-fed mice and treated with or without recombinant CysC (n=5 independent experiments). Values are expressed as mean±SEM. #p=0.06 (A), #p=0.09 (B), *p<0.05, **p<0.01, ***p<0.001. Student's *t*-test.

Fig. 4 Negative correlation of circulating CysC levels with inflammation markers in human WAT

Scatter plot and correlation coefficient (r) of *log* circulating CysC concentration and subcutaneous WAT *HIF1α* (A), subcutaneous WAT *TNFα* (B), visceral WAT *HIF1α* (C) and visceral WAT *IL-6* (D) mRNA expression (n=62-63). Scatter plot and correlation coefficient (r) of *log* circulating CysC concentration and serum lipocalin-2 (E) or serum IL-10 (F) concentration (n=42-44). (G) *CysC* mRNA expression in subcutaneous WAT of insulin-sensitive and insulin-resistant healthy obese patients (n=30 patients per group). *p<0.05, (Student's *t*-test).

Figure 1

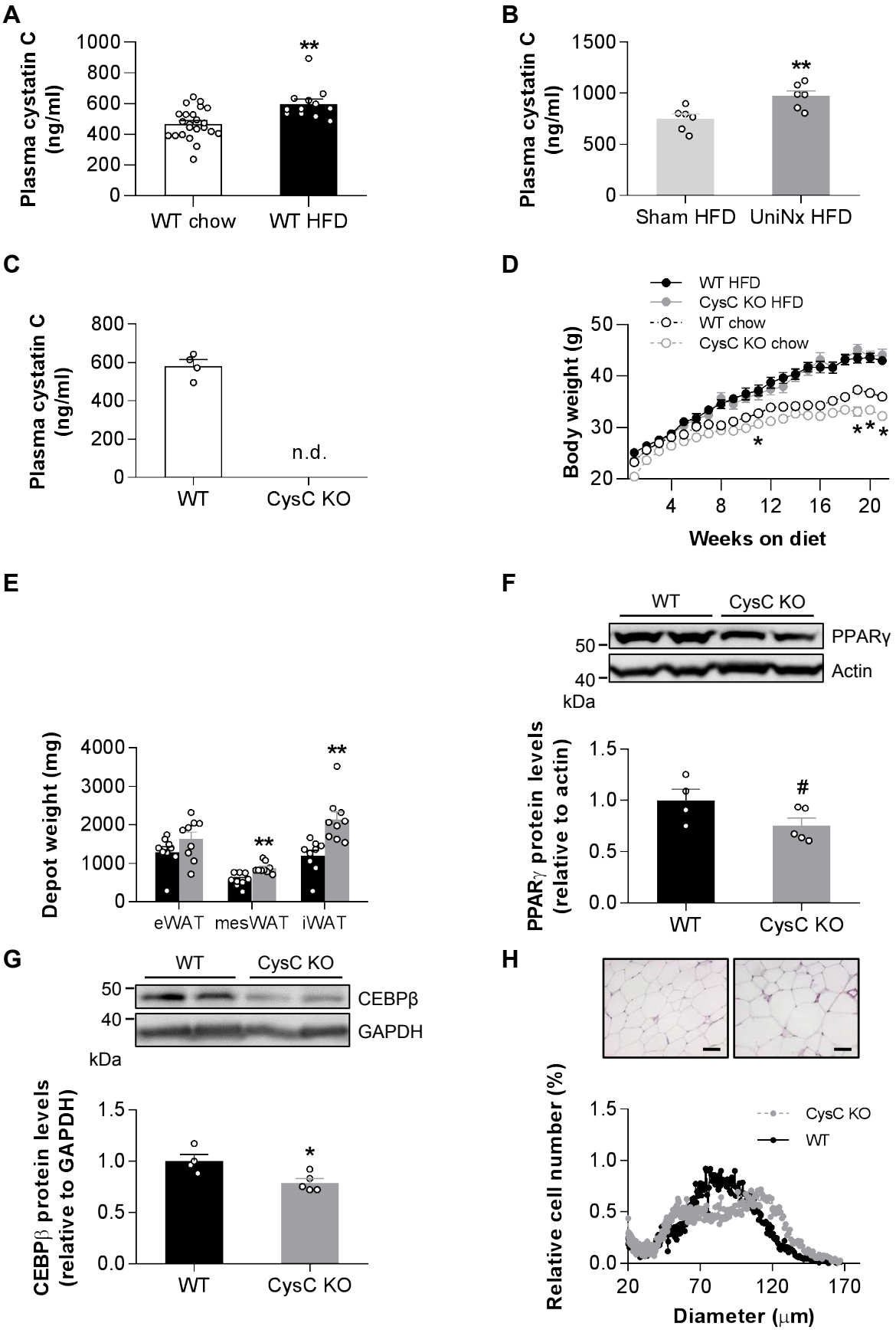
A
Plasma cystatin C (ng/ml)
1000
800
600
400
200
0
**
WT chow
WT HFD
B
Plasma cystatin C (ng/ml)
1500
1000
500
0
**
Sham HFD
UniNx HFD
C
Plasma cystatin C (ng/ml)
800
600
400
200
0
n.d.
WT
CysC KO
D
WT HFD
CysC KO HFD
WT chow
CysC KO chow
Body weight (g)
50
40
30
20
*
**
4
8
12
16
20
Weeks on diet
E
Depot weight (mg)
4000
3000
2000
1000
0
**
**
eWAT
mesWAT
iWAT
F
WT
CysC KO
50
40
kDa
PPARγ
Actin
PPARγ protein levels (relative to actin)
1.5
1.0
0.5
0.0
#
WT
CysC KO
G
WT
CysC KO
50
40
kDa
CEBPβ
GAPDH
CEBPβ protein levels (relative to GAPDH)
1.5
1.0
0.5
0.0
*
WT
CysC KO
H
Relative cell number (%)
1.5
1.0
0.5
0.0
CysC KO
WT
20
70
120
170
Diameter (μm)

Figure 2

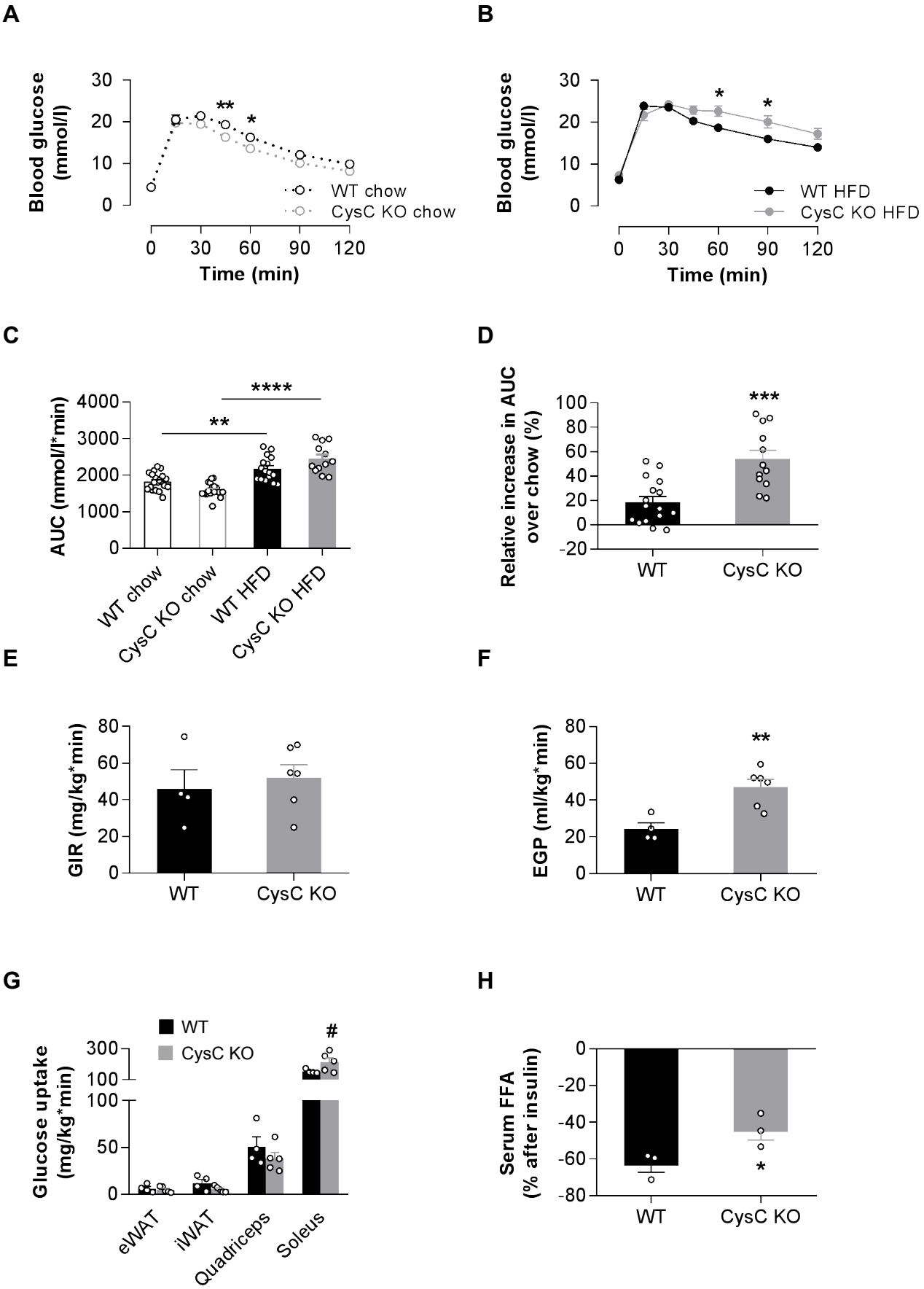
A
Blood glucose (mmol/l)
30
20
10
0
**
*
WT chow
CysC KO chow
0
30
60
90
120
Time (min)
B
Blood glucose (mmol/l)
30
20
10
0
*
*
WT HFD
CysC KO HFD
0
30
60
90
120
Time (min)
C
AUC (mmol/l*min)
4000
3000
2000
1000
0
**
****
WT chow
CysC KO chow
WT HFD
CysC KO HFD
D
Relative increase in AUC over chow (%)
100
80
60
40
20
0
-20
***
WT
CysC KO
E
GIR (mg/kg*min)
80
60
40
20
0
WT
CysC KO
F
EGP (ml/kg*min)
80
60
40
20
0
**
WT
CysC KO
G
Glucose uptake (mg/kg*min)
WT
CysC KO
300
100
100
50
0
#
eWAT
iWAT
Quadriceps
Soleus
H
Serum FFA (% after insulin)
0
-20
-40
-60
-80
*
WT
CysC KO

Figure 3

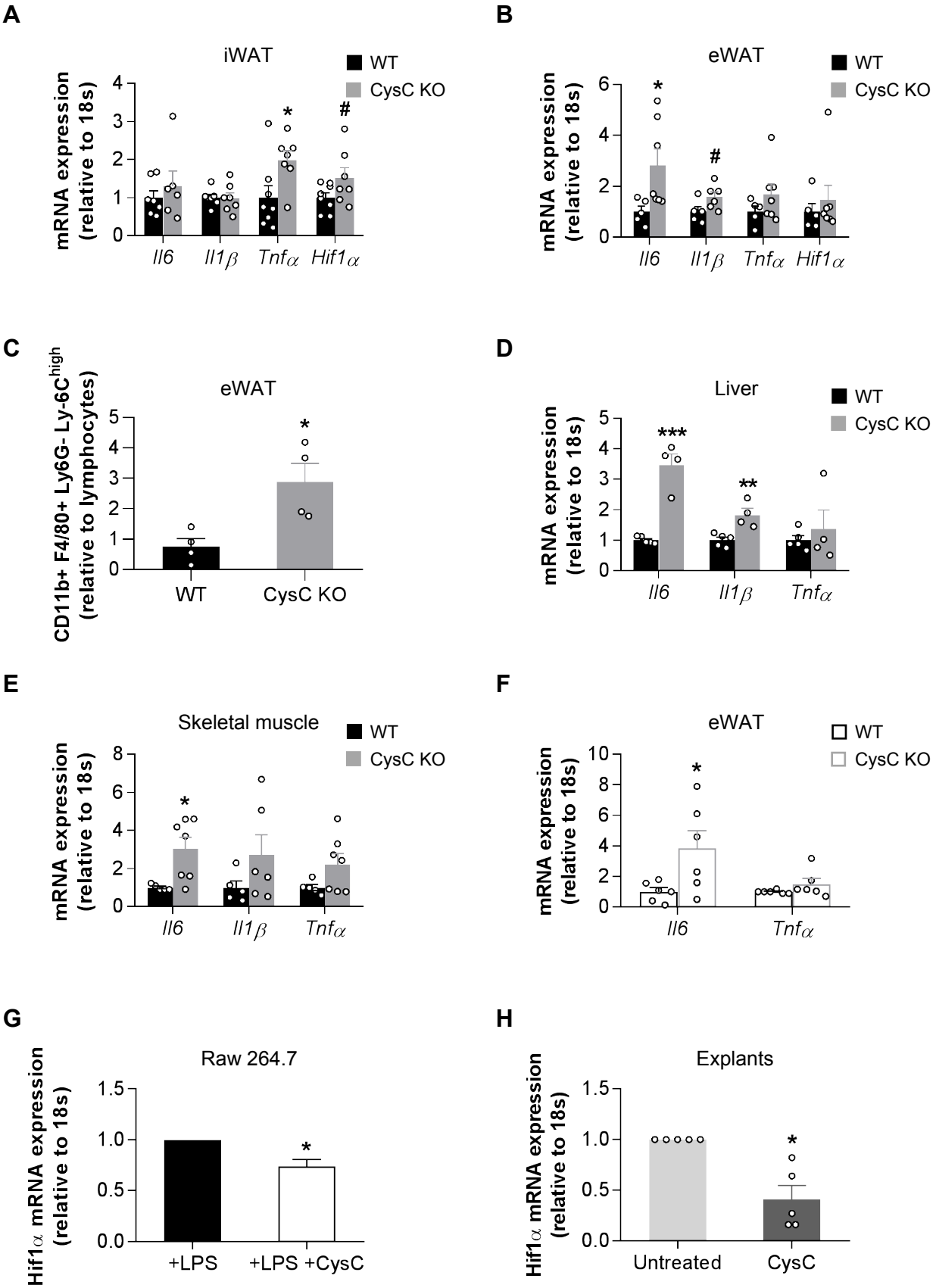
A
iWAT
WT
CysC KO
mRNA expression (relative to 18s)
Il6
Il1β
Tnfα
Hif1α
B
eWAT
C
CD11b+ F4/80+ Ly6G- Ly-6C^high (relative to lymphocytes)
D
Liver
E
Skeletal muscle
F
eWAT
G
Raw 264.7
Hif1α mRNA expression (relative to 18s)
+LPS
+LPS +CysC
H
Explants
Untreated
CysC

Figure 4

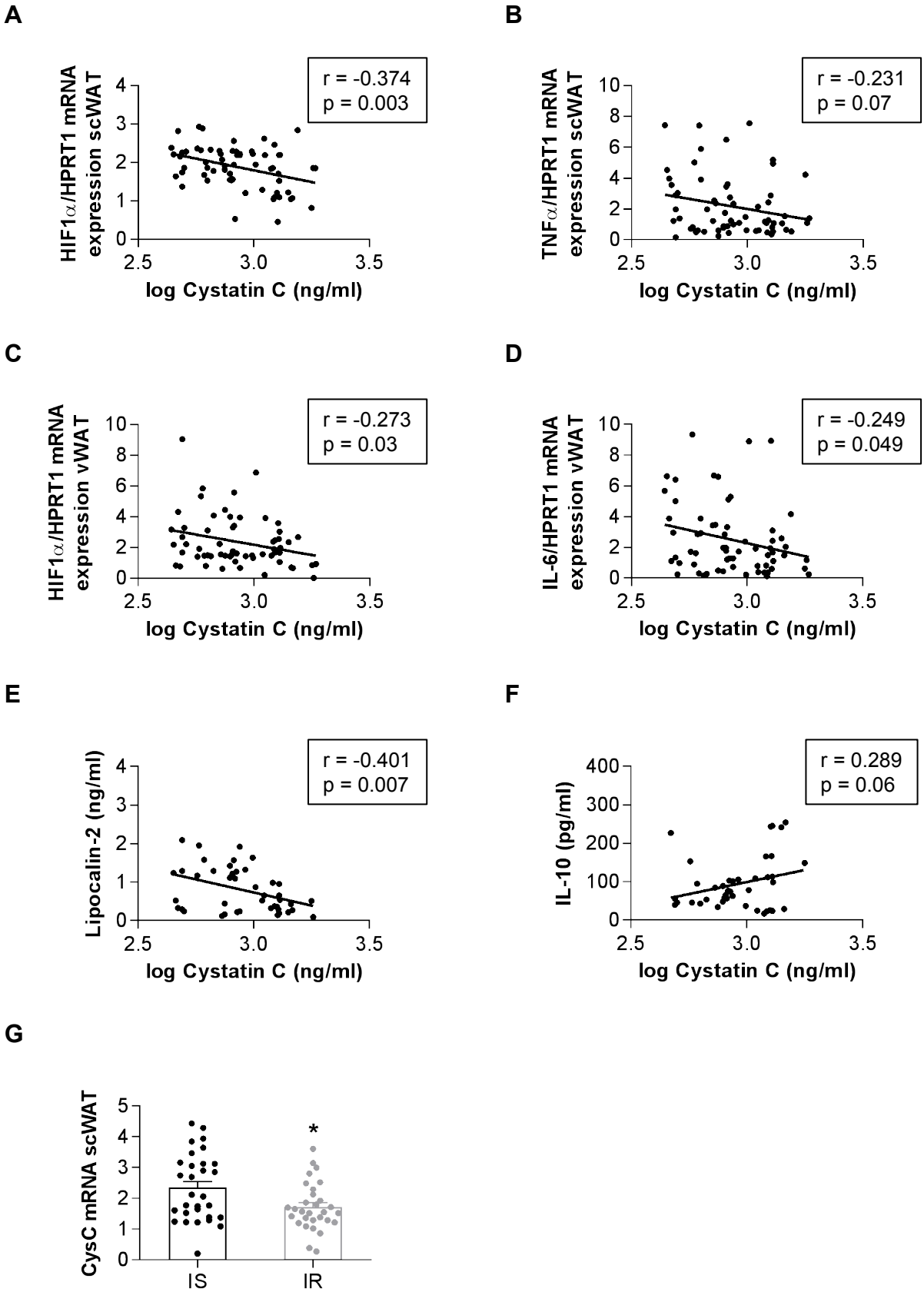
A
HIF1α/HPRT1 mRNA expression scWAT
r = -0.374
p = 0.003
log Cystatin C (ng/ml)
B
TNFα/HPRT1 mRNA expression scWAT
r = -0.231
p = 0.07
log Cystatin C (ng/ml)
C
HIF1α/HPRT1 mRNA expression vWAT
r = -0.273
p = 0.03
log Cystatin C (ng/ml)
D
IL-6/HPRT1 mRNA expression vWAT
r = -0.249
p = 0.049
log Cystatin C (ng/ml)
E
Lipocalin-2 (ng/ml)
r = -0.401
p = 0.007
log Cystatin C (ng/ml)
F
IL-10 (pg/ml)
r = 0.289
p = 0.06
log Cystatin C (ng/ml)
G
CysC mRNA scWAT
*
IS
IR

Obesity-Induced Increase in Cystatin C Alleviates Tissue Inflammation

Mara A. Dedual, Stephan Wueest, Tenagne D. Challa, Fabrizio C. Lucchini, Tim R. J. Aeppli, Marcela Borsigova, Andrea A. Mauracher, Stefano Vavassori, Jana Pachlopnik Schmid, Matthias Blüher, Daniel Konrad

Supplementary Figures 1-11

Supplementary Tables 1-4

Supplementary Figure 1

A

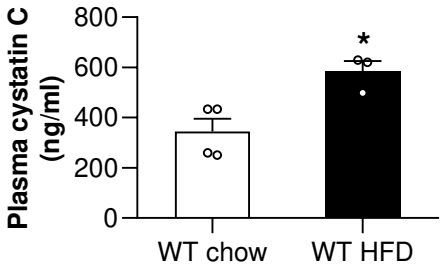

B

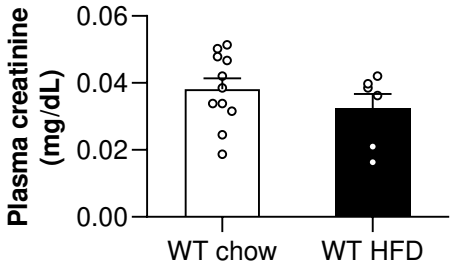

Increased circulating cystatin C levels in HFD-fed mice

(A) Plasma levels of cystatin C in portal blood of WT mice (n=4 chow-fed mice and n=3 HFD-fed mice). (B) Plasma levels of creatinine in systemic blood of chow- and HFD-fed WT mice (n=11 chow-fed mice and n=6 HFD-fed mice). Values are expressed mean±SEM. *p<0.05 (Student's *t*-test).

Supplementary Figure 2

A

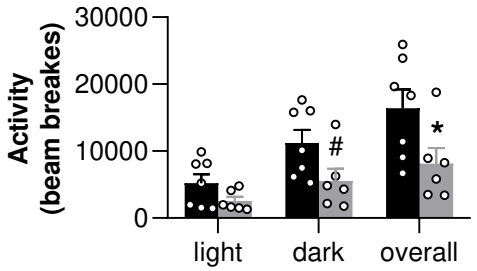

B

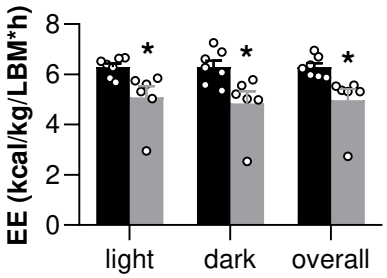

C

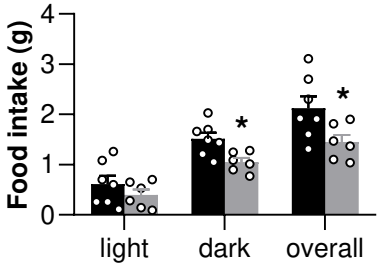

Decreased locomotor activity, energy expenditure and food intake in HFD-fed CysC KO mice

(A) Locomotor activity, (B) energy expenditure and (C) food intake of HFD-fed WT and CysC KO mice (n=7 WT and n=6 CysC KO mice). Values are expressed as mean±SEM. (A) #p=0.06. *p<0.05 (Student's *t*-test).

Supplementary Figure 3

A

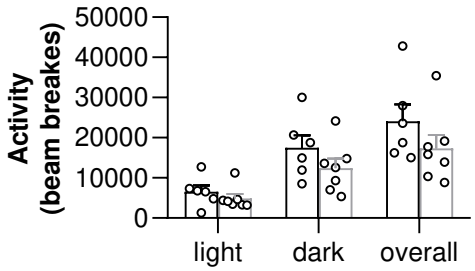

B

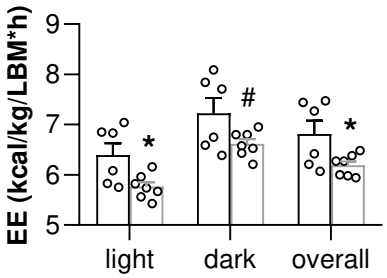

C

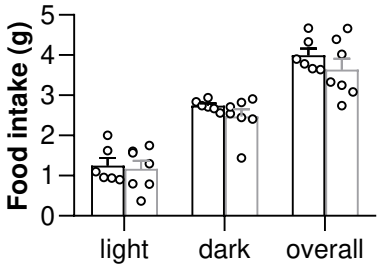

Similar locomotor activity and food intake, but decreased energy expenditure in chow-fed CysC KO mice

(A) Locomotor activity, (B) energy expenditure and (C) food intake of chow-fed WT and CysC KO mice (n=6 WT and n=7 CysC KO mice). Values are expressed as mean±SEM. $^{\#}p=0.06$, *p<0.05 (Student's *t*-test).

Supplementary Figure 4

A

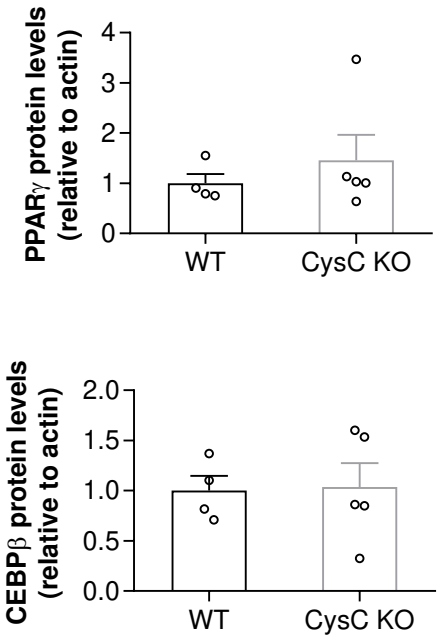

B

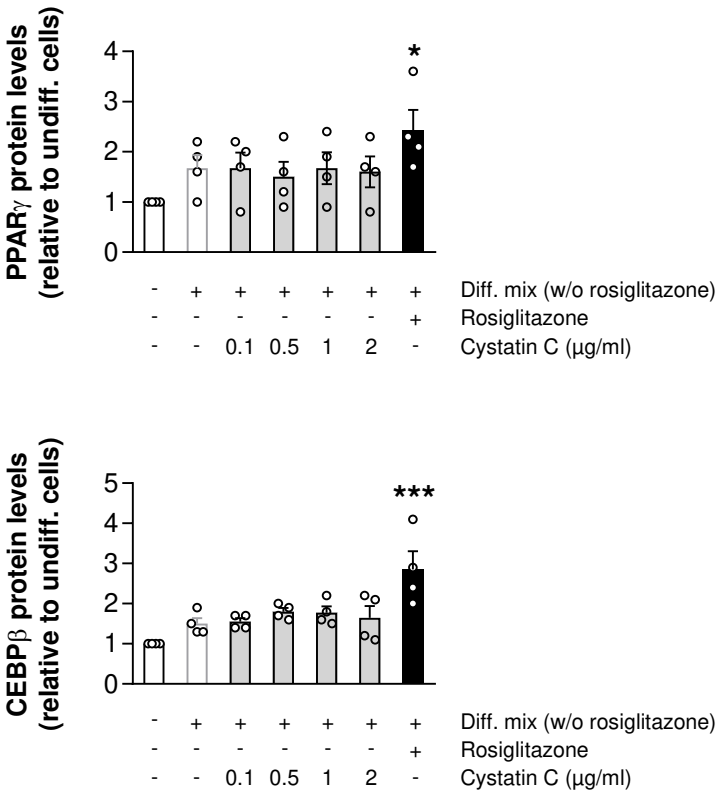

No effect of recombinant CysC on 3T3-L1 adipocyte differentiation

(A) Quantification of protein levels of PPARγ and CEBPβ in iWAT of chow-fed WT (n=4) and CysC KO (n=5). Protein levels were normalized to WT mice. (B) Confluent 3T3-L1 adipocytes were treated for three days with or without a differentiation (Diff.) mix containing 500 µM isobutylmethylxanthine, 1 µM dexamethasone and 1.7 µM insulin, rosiglizatone (1µM) and different concentrations of recombinant CysC as indicated. Thereafter, cells were treated for three days with or without a second Diff. mix containing 0.5 µM insulin and different concentrations of recombinant CysC as indicated. Six days after induction of differentiation, cells were lysed and Western blots were performed. Shown are quantified protein levels of PPARγ and CEBPβ. n=4 biological replicates. Values are expressed as mean±SEM. *$p<0.05$, ***$p<0.001$ (ANOVA, compared to undifferentiated cells).

Supplementary Figure 5

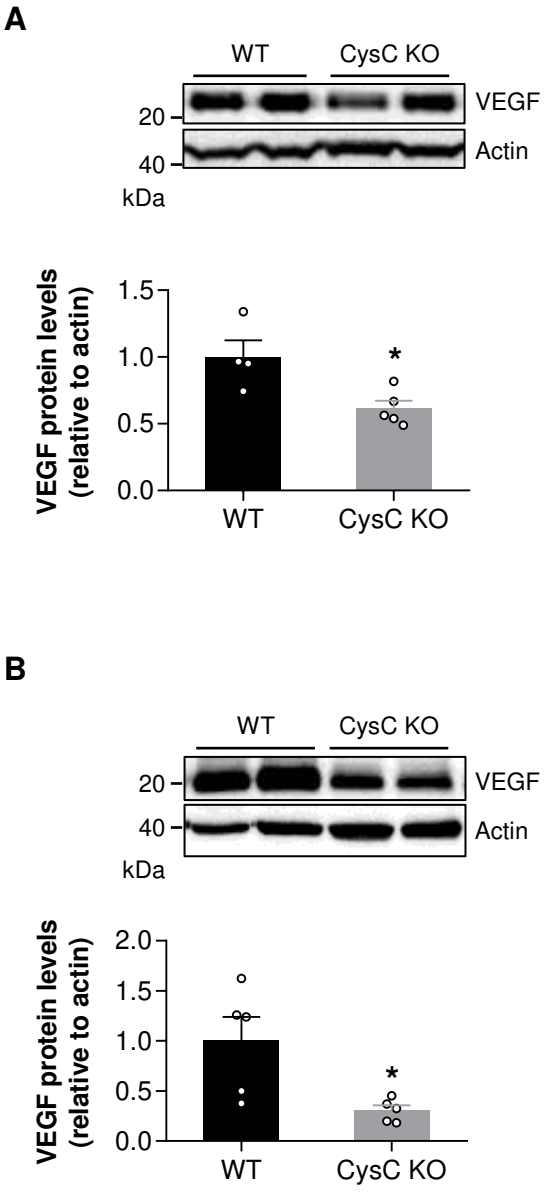

Decreased VEGF levels in skeletal muscle of HFD-fed CysC KO mice

Representative Western blots and quantification of protein levels of VEGF in iWAT (A; n=4 WT and n=5 CysC KO) and in skeletal muscle of HFD-fed mice (B; n=5 mice per group). Protein levels were normalized to WT mice. Values are expressed as mean±SEM. *p<0.05 (Student's *t*-test).

Supplementary Figure 6

A

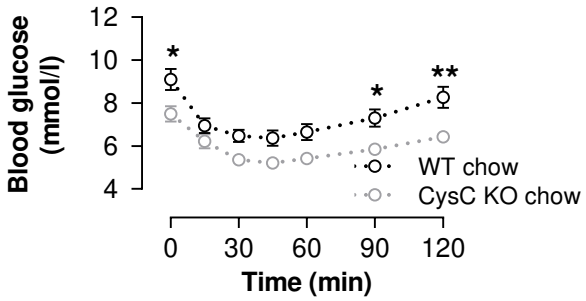

B

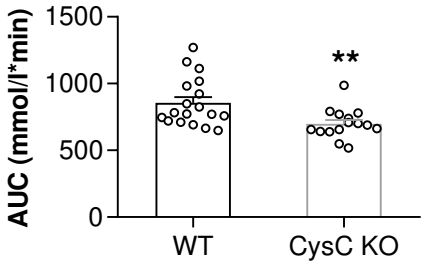

C

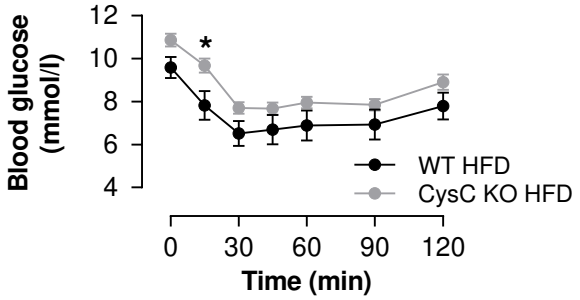

D

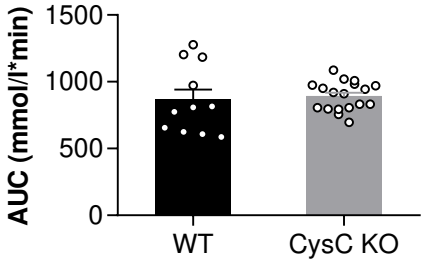

E

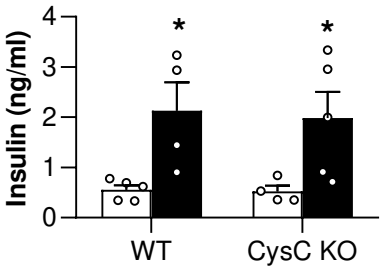

Insulin tolerance in chow- and HFD-fed WT and CysC KO mice

Intraperitoneal insulin tolerance test (ipITT) in chow- (n=18 WT and n=15 CysC KO mice) and HFD-fed (n=11 WT and n=18 CysC KO mice) WT and CysC KO mice (A-D). (E) Circulating insulin levels of chow- and HFD-fed WT mice (chow n=5, HFD n=4) as well as CysC KO mice (chow n=4, HFD=5). Values are expressed as mean±SEM. *p<0.05, **p<0.01. Student's *t*-test (B, D, E), two-way ANOVA (A, C).

Supplementary Figure 7

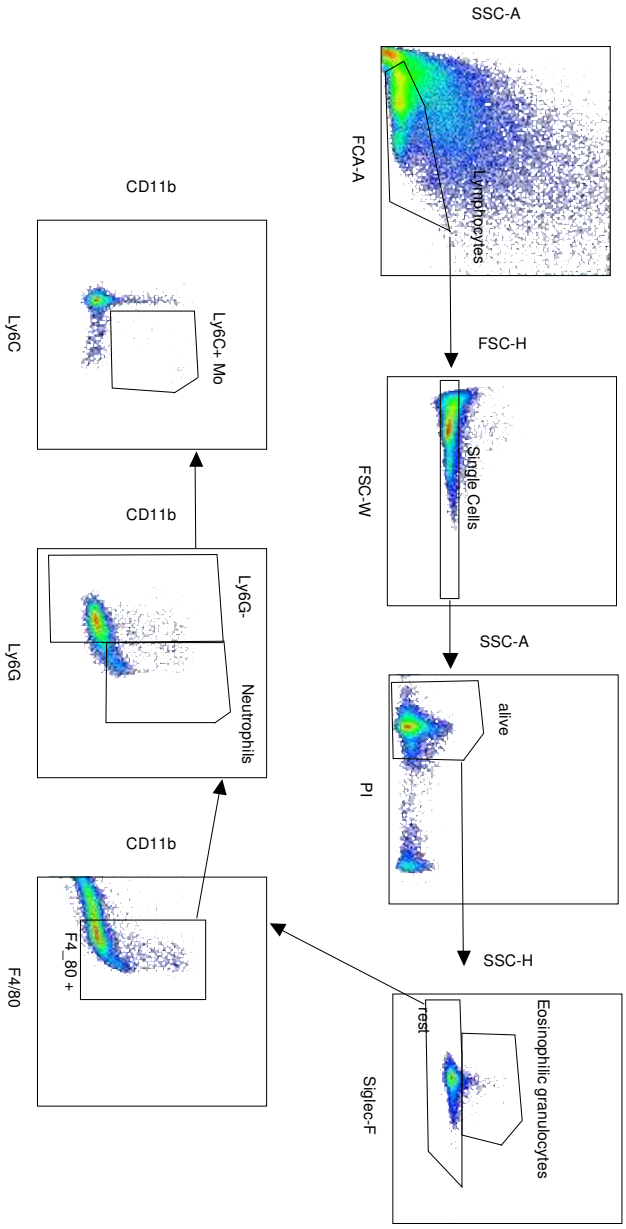

Gating strategy on cells in eWAT

Lymphocytes and single cells were initially identified by size. PI negative cells were identified as alive. Following exclusion of Eosinophils we gated on F4/80. Afterwards Ly6G negative cells were gated on macrophages based on CD11b and Ly6C expression. PI: Propidium iodide.

Supplementary Figure 8

A

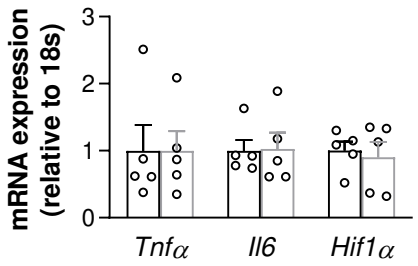

B

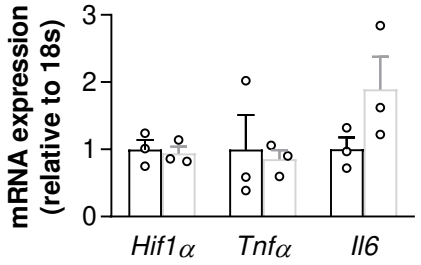

C

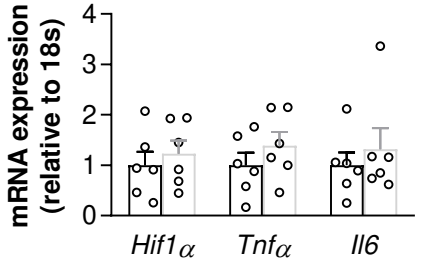

Similar expression of pro-inflammatory cytokines in WAT of chow-fed WT and CysC KO mice

mRNA expression levels of pro-inflammatory cytokines in (A) eWAT (n= 5 mice per group), (B) Liver (n=3 per group) and (C) skeletal muscle (n=6 per group) of chow-fed WT and CysC KO. Values are expressed as mean±SEM.

Supplementary Figure 9

A

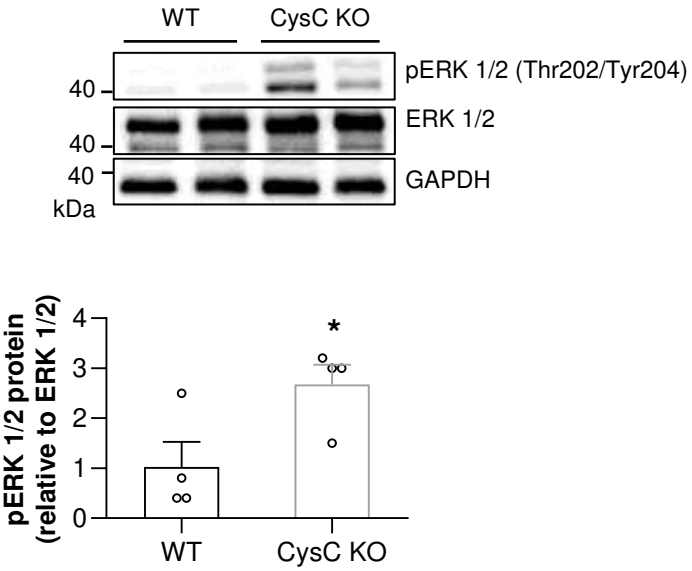

B

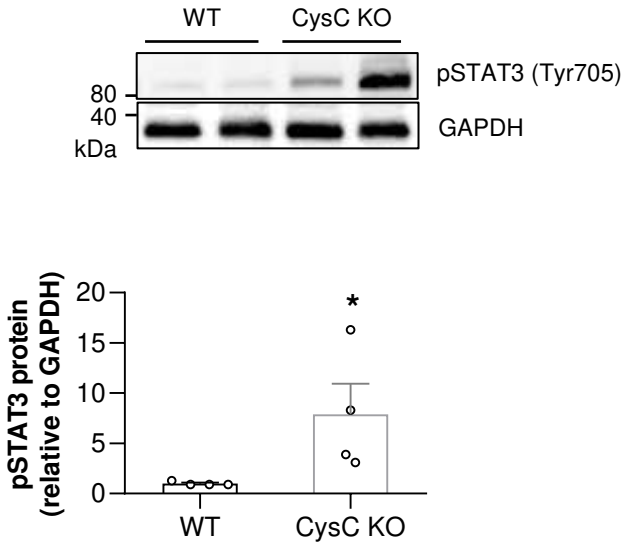

Increased ERK and STAT3 phosphorylation in adipose tissue of LPS-treated CysC KO mice

Phosphorylation levels of selected IL-6 downstream targets ERK 1/2 (A) and STAT3 (B) (n=6 mice per group). Values are expressed mean±SEM. *p<0.05 (Student's *t*-test).

Supplementary Figure 10

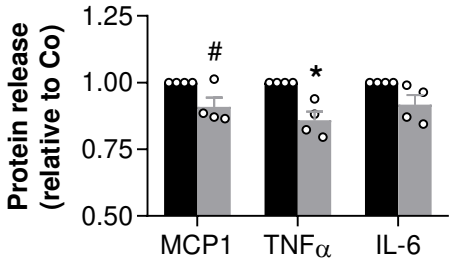

Decreased release of pro-inflammatory mediators from CysC-treated RAW cells
MCP1, TNFα and IL-6 protein levels were determined in the supernatant of LPS-stimulated RAW 264.7 cells in the absence (controls (Co), black bars) or presence of CysC (grey bars). Protein release was normalized to RNA concentration and is shown relative to Co cells. n=4 independent experiments. $^{\#}p<0.1$, $^{*}p<0.05$ (One sample *t*-test).

Supplementary Figure 11

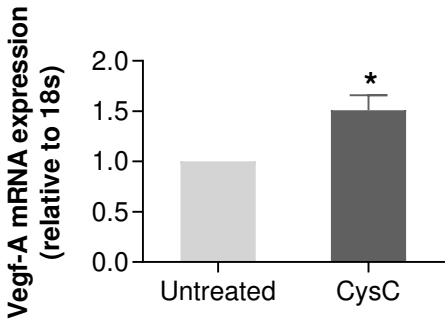

Increased *Vegf-A* expression in cystatin C-treated eWAT explants

mRNA expression of *Vegf-A* in eWAT explants harvested from HFD-fed mice and treated with or without recombinant cystatin C (n=5 independent experiments). Values are expressed mean±SEM. *p<0.05 (Student's *t*-test).

Supplementary Tab. 1 mRNA primer used for experiments in human individuals

mRNA	*Order number*
HIF1α	Hs00153153_m1
TNFα	Hs01113624_g1
IL-6	Hs00985639_m1
CysC	Hs00264679_m1
HPRT1 mRNA	Hs01003267_m1

Primers were provided by Applied Biosystems, Darmstadt, Germany

Supplementary Tab. 2 mRNA primer used for experiments in mice

mRNA	*Order number*
Hif1α	Mm00468869_m1
Tnfα	Mm00443258_m1
Il-6	Mm00446190_m1
Vegf-A	Mm01281449_m1

Primers were provided by Applied Biosystems, Rotkreuz, Switzerland

Supplementary Tab. 3 Order number of primary antibodies used

Target	*Order number*	*Company*
Actin	MAB1501	Millipore, Billerica, MA, USA
CEBPβ	sc-150	Santa Cruz Biotechnology, Dallas, TX, USA
PPARγ	sc-7196	Santa Cruz Biotechnology
pSTAT3 (Tyr705)	D3A7	Santa Cruz Biotechnology
VEGF	sc-7269	Santa Cruz Biotechnology
ERK 1/2	9102	Cell Signaling Technology, Danvers, MA, USA
pERK 1/2 (Thr202/Tyr204)	9101	Cell Signaling Technology
GAPDH	10494-1-AP	Proteintech, Rosemont, IL, USA

Supplementary Tab. 4 Dye and fluorochrome-coupled antibodies used for flow cytometry

Antibody	*Company*
fluorescein isothiocyanate (FITC)–anti-Annexin	BioLegend Way, San Diego, CA, USA
phycoerythrin (Pe)/Cy7–anti-CD11b (clone M1/70)	BioLegend Way
PE–anti-Ly6G	BioLegend Way
APC-Cy7–anti-Ly6C (clone HK1.4)	BioLegend Way
Biotin–anti-Siglec-F	BioLegend Way
Alexa Fluor 700–streptavidin	BioLegend Way
APC–anti-F4/80	BioLegend Way